(4)

OFFICE OF NAVAL RESEARCH

Contract N0001488WX24207

TECHNICAL REPORT NO. 1

Anomalous Fatigue Behavior in Polyisoprene

by

C. M. Roland
Naval Research Laboratory
Chemistry Division, Code 6120
Washington, DC 20375-5000

and

J. W. Sobieski
Geo-Centers, Inc.
Fort Washington, MD 20744

Presented at the 134th Meeting
Rubber Division, American Chemical Society
Cincinnati, Ohio
October 18-21, 1988

INTRODUCTION

Material failure corresponds to the propagation of damage to a catastrophic level. The damage may be intrinsic or have arisen during deformation. In cross-linked rubbers it is known that even the most carefully prepared laboratory specimens have inherent flaws which are capable of initiating crack growth. Fracture is made possible when the strain energy release rate (i.e., the tearing energy) exceeds a critical value. This tearing energy is defined as [1-3]

$$T = -t^{-1} \, (dU / dc) \qquad (1)$$

where t is the specimen thickness, U the stored energy, and c the crack length. The value of T associated with catastrophic failure is a material property referred to as the fracture energy or tear strength. The tensile strength or breaking stress of the material is the stress at which the strain energy release rate attains this critical value. Below the level of tearing energy necessary for catastrophic failure, mechanical crack propagation proceeds at a finite rate (e.g., per number of cycles, N) that can often be described by a power law relation

$$dc/dN = aT(c)^b \qquad (2)$$

where a and b are presumed material constants. When the tearing energy is insufficient for mechanical crack growth, in unsaturated rubbers chemically induced chain scission (e.g., by

reaction with ozone) transpires at a rate that is essentially independent of the tearing energy.

For a tensile deformation, equation (1) takes the form

$$T = 2kUc/V \qquad (3)$$

where V is the volume of deformed material and k a geometric factor that depends weakly on the elongation, e [3]

$$k = (1 + e)^{-1/2} \qquad (4)$$

The magnitude of the strain energy release rate for tensile straining thus increases in proportion to the extent of crack growth, so that the rate of crack propagation accelerates rapidly ($b > 2$). Before cracks of visible size (circa 0.1 mm) have formed, a majority of the total cycles required for failure have transpired. The fatigue lifetime, N_f, or number of deformation cycles required for the inherent flaw size, c_o, to grow to the critical magnitude, c_c, for catastrophic failure, is [3,4]

$$N_f = a^{-1} \int_{c_o}^{c_c} T(c)^{-b}\, dc \qquad (5)$$

For tensile deformation

$$N_f = (a-ab)^{-1}\ (2kU/V)^{-b}\ c_o^{1-b} \qquad (6)$$

since $c_c >> c_o$.

The attraction of the tearing energy approach to material fatigue and fracture arises from the assumption that the tear energy dependence of the crack propagation rate is a material property, independent of the particular test geometry employed for measurements. This allows life predictions to be made for materials subjected to a complicated or difficult to simulate deformation, provided the strain energy release rate for the deformation can be deduced.

Notwithstanding the success in its application to many failure problems in rubber, there are limitations to the tearing energy approach. Of questionable general validity is the assumption that the volume of material in immediate proximity to the crack front simply translates without change with the propagating crack. This highly stressed region has been shown to be replete with microcracks [5]. The nature of their accumulation is largely unexplored, but it has been demonstrated that the chemical composition of the material and the details of the deformation process influence the structure of the microdamage [5]. Fracture below T_g or in semi-crystalline materials is well known to reflect the evolution into new crack surfaces of the micro-damaged material surrounding the crack [6-8]. The significance of damage evolution in the fracture of elastomers is unknown.

Any influence of the imposed strain cycle on the induction of crystallization in the polymer is also neglected in the simple

fracture mechanics approach to rubber failure. An example of this failing of the tear energy criterion to account for crack growth behavior is when the minimum amplitude of the strain cycle is increased from zero ("relaxing" cyclic deformation) to some non-zero magnitude ("non-relaxing" deformation). While such a change has negligible effect on the crack propagation rate of a non-crystallizing elastomer, the crack growth resistance of a material capable of strain induced crystallization is markedly improved under this circumstance [9]. The strain induced crystallization at the crack tip enhances the resistance to fracture and thus stabilizes the crack.

This report is concerned with the effect on the fatigue life and other failure properties of rubber of imposition of a period of annealing in a strained state.

EXPERIMENTAL

The cis-1,4-polyisoprene was either Hevea Brasiliensis, NR (SMR-L from the Ore and Chemical Corporation) or the synthetic variant, IR (Natsyn 2210 from the Goodyear Tire and Rubber Co.), and the styrene-butadiene copolymer was solution SBR with 22.5% styrene (Duradene 706 from the Firestone Tire and Rubber Company). Stock formulations are given in Table I. Mixing was carried out on a two roll mill, except for those stocks containing carbon black, which were initially mixed in a Brabender Prep Center. Curing was executed at 160^{o}C for 30 minutes in all cases.

Using an Instron 4206, uniaxial deformation data was obtained both at 0.1 sec^{-1} and in equilibrium. For the latter the test specimen was elongated to the desired strain and the force measured continuously during the subsequent stress relaxation. When no further reduction in force was detected over a 30 minute time period, the specimen elongation was increased. Typically elastic equilibrium measurements were made every 10% elongation up to failure. All cross head motions were controlled using a Hewlett Packard 216 microcomputer. Stress relaxation behavior was characterized using an Imass Corp. Dynastat Mark II instrument. Following imposition of a deformation the stress was typically monitored over a time period of from 10^{-2} to 10^{4} seconds.

Tensile fatigue testing was conducted along the lines of ASTM D4482-85 using a Monsanto Fatigue To Failure Tester. In this procedure the specimens are cycled a few hundred times, after which the "set" that developed is removed by displacement of the test fixture cross-head. The minimum of the dynamic fatigue deformation thus corresponds to zero stress. The instrument was modified to enable accurate counting of fatigue cycles. In order to avoid errors due to switch bounce, the counters were replaced with a parallel interface board. In conjunction with a microcomputer, this enabled the condition of each microswitch to be monitored a few times each millisecond, so that erroneous readings could be detected. The maximum amplitude of the dynamic deformation was typically 124% elongation. As

described below, in some cases the testing was interrupted after a number of cycles and the specimens annealed under different conditions for various durations. A minimum of eight specimens were used per test. Cut growth measurements were obtained from initially precut specimens deformed in tension with a Haversine waveform using an MTS apparatus.

Except where noted, all experimentation was carried out at room temperature.

RESULTS

There is no expectation that the fatigue lifetime of a rubber will be affected by intermittent cessation of the cyclical deformation. For example, as seen in Table II, fatigue lifetimes for constant strain deformation differ insignificantly between uninterrupted fatigue cycling versus cycling during which an extended "rest" period (in an unstrained state) was imposed at some point during the course of the cycling.

In Table III are displayed fatigue lifetimes for an IR based stock measured according to the ASTM D4482-85 procedure. The creep (or set) developing in the test specimens was removed after 200 cycles so that the minimum of the strain cycle corresponded to zero stress without buckling. In some cases the fatigue deformation was halted after a number of cycles and the test specimens maintained at either the maximum or minimum dynamic strain amplitude for a time period, followed by resumption of the fatigue testing. This interruption of the cycling markedly altered the fatigue results (Table III). Crack propagation,

although usually associated with cyclical deformation, is nevertheless known to transpire when an elastomer is maintained in a constant (no cycling) strained state. While it might therefore be expected that reduction in the number of deformation cycles required for failure would accompany the imposition of a period of constant strain in the course of the usual fatigue experiment, the behavior illustrated in Table III is more complicated. Annealing at elevated strain (e.g., 124% elongation) increased the fatigue lifetime relative to the results for uninterrupted fatigue testing. Such improvement was typically observed after 24 hours or more annealing at 124% extension. On the other hand, when the annealing was executed at the minimum of the strain cycle (corresponding to zero dynamic stress) there was a dramatic decrease in the total number of fatigue cycles required for failure. Similar fatigue results were obtained both with NR based stocks and with filled compounds (Table IV). The improvements in fatigue life accompanying annealing at high strain, as well as the reduction in lifetime due to annealing at the minimum dynamic strain amplitude, are significant, notwithstanding the large scatter inherent in failure property measurements (see Figure 1).

As discussed above, fatigue and tensile strength reflect identical phenomena - the growth of flaws and concurrent (at least for uniaxial extension) increase in tearing energy up to the point of failure. Accordingly it is useful to assess in comparison to the fatigue results the effect on tensile strength

of annealing in various states of strain. Displayed in Figure 2 is the tensile strength measured for NR-2 annealed 72 hours at various strains. Two characteristic features are in evidence. At low annealing elongations (ca. 10%) a minimum in tensile strength is attained. As the strain during annealing is increased, there is a corresponding increase in the subsequently measured breaking stress. At sufficiently high annealing strains the strength is actually greater than the original (unannealed) tensile strength.

Fatigue Life Reduction

In contrasting the fatigue and strength results, we note that during fatigue cycling the adjustment to remove buckling of the test specimens due to unrecovered strain (the "set") was equivalent to 12% strain. Although exact correspondence would be coincidental, it is instructive that the minimum in Figure 2 occurs in proximity to the dynamic strain during cyclic deformation associated with zero stress. The annealing during the fatigue experiments was conducted at this minimum dynamic strain; however, the stress does not remain zero when the fatigue cycling ceases. In Figure 3 are shown stress relaxation measurements for the NR-2 after imposition of a double step strain. The time required for no significant further decay of stress is on the order of 10^2 seconds. In the range of linear viscoelastic behavior, it is to be expected that when a sample is maintained after cessation of cycling at the strain corresponding to zero dynamic stress, the stress will build up to the static

equilibrium value in roughly 10^2 seconds. In the presence of reversing strain cycles, however, cross-linked rubber diverges from linear viscoelastic behavior at strains well within the domain of linearity as judged by the usual methods (e.g., strain independence and time invariance of the mechanical response) [10]. As seen in Figure 3, after a double step strain in which the strains differ in sign a stress undershoot is observed (congruent with a "permanent set"), after which the elastic equilibrium stress is attained in a time period dependent upon the duration of the initial strain. The set is actually not permanent, and recovers over a time scale dependent on the duration of the initial step loading. The non-zero strain at zero stress (and negative load at zero strain if the specimen does not buckle) is due to inhomogeneous deformation on the molecular level, with network strands present in both extended and compressed configurations [10]. Thus, when imposed during the course of a dynamic fatigue experiment, annealing at the "permanent set" strain is equivalent to annealing at a stress that increases in time. A static stress level is attained in a time period dependent upon the dwell time at the previous higher strain (Figure 3).

The origin of the reduction in fatigue performance when the specimens are maintained at the minimum dynamic strain is clearly due to processes induced by annealing at low static stresses. The minimum in tensile strength as a function of annealing strain is similarly seen in both IR and SBR based rubbers (Figure 4 and

5 respectively). This annealing does not measurably alter the cross-link density (Table V), suggesting that the changes in failure properties is not due to a bulk effect.

At annealing strains greater than those associated with the minimum in failure properties, the samples exhibit a readily apparent whitening. Scanning electron micrographs reveal this whitening to be due to extensive cracking at the surface of the specimens (Figure 6). Contrarily, after annealing at low strains (ca. 10%) even for several days no whitening of the samples arises, although surface cracks visible to the naked eye become evident. At higher annealing strains, such large cracks never appear. As annealing at higher strains (>20%) is continued, the region of the material with an abundance of small (on the order of a micron) surface cracks extends progressively deeper into the rubber. For example, for the NR-2 it was determined from scanning electron micrographs that the thickness of the damage zone at the surface increased from about 7 microns after 24 hours to over 30 microns after three days. The severity of the surface damage also increases over the first couple of days, although after this its progression into the bulk of the sample slows noticeably.

When the annealing of test specimens is executed in vacuum, there is no large reduction in fatigue life or strength of the rubber, nor does surface cracking transpire. From this and the observation that the cracking in air is confined to the surface, it is clear that the damage accumulating during the course of

annealing is due to chemical attack, specifically reaction with ozone. It is known that ozone readily reacts with unsaturated hydrocarbons [11,12], and the ambient ozone concentration was evidently significant. When the strain is low, the strain energy release rate, which for uniaxial extension is proportional to the product of crack length and strain (equation 3), is sufficient to effect ozone cracking only for the largest flaws present. These larger flaws thus grow in size with a concomitant reduction in fatigue life or strength of the rubber. At higher annealing strains, the strain energy is high enough that many of the cracks initially present experience the strain energy release rate necessary for stress induced ozone cracking. The high concentration of microcracks causes their mutual interference. These surface flaws do not amplify the stress because neighboring cracks have released the strain energy of the material at the crack tips. Annealing at low strains is more deleterious than that done at high strains because only the largest flaws determine the failure properties. Note that the extensive damage originating at the surface when the annealing is done at higher strains does not per se reduce the strength since this damage region represents only a small fraction (1 or 2 %) of the total material. Strain amplitude effects such as these on the nature of ozone cracking have been previously described by various investigators [13-16]. The influence of annealing at low strains during the course of a fatigue experiment is an equivalent phenomenon upon recognition that the zero stress at the minimum

in the dynamic straining becomes non-zero upon cessation of the cycling.

It is interesting to note, however, that the fraction of the fatigue life transpiring prior to annealing has a significant influence on the ultimate behavior. Displayed in Figure 7 is the tensile strength measured after annealing at various strains for 72 hours in air. The curves represent different extents of cycling prior to imposition of the annealing. A minimum in the dependence of the strength on annealing strain is observed when as many as 40,000 cycles are executed prior to annealing. If a greater fraction of the lifetime has expired before annealing, however, annealing has no significant effect on the subsequently measured tensile strength. To explain this phenomenon, it is necessary to consider the nature and growth of the flaws initially present in the material. When the tip radius of the crack is much smaller than its length, the stress intensification in an elastic material will be directly proportional to the square root of the length [3,17]. This means that the breaking stress should vary in inverse proportion to the length of the flaw. Notwithstanding significant deviations from elastic mechanical behavior, this relationship between flaw size and tensile strength has been verified for rubber [3]. Displayed in Figure 8 is the tensile strength measured for NR-2 samples in which razor cuts of various length were introduced into the edge of the specimens. For sufficiently large precuts, the tensile strength drops markedly due to the absence of strain induced

crystallization [18,19]. For smaller initial cuts, the expected proportionality of the tensile strength to the inverse square root of the (optically measured) flaw size is observed. By extrapolating this linear portion of the curve to the measured strength of uncut specimens, a value of 70 microns is deduced for the maximum inherent flaw size. From the dependence of the crack growth propagation rate (expressed as meters per cycle) on tearing energy (in MJ per square meter), measured to be

$$dc/dN = 2 \times 10^{-7} T^3 \qquad (7)$$

the length of the largest flaws after a given duration of fatigue cycling can be estimated. Using equations 5 and 7, this crack length is found to vary according to

$$c(N) = (4.2 \times 10^{16} - N/2.1 \times 10^{-12})^{-1/4} \qquad (8)$$

Applying equation 8 it is seen that, whereas the first 40,000 fatigue cycles only increase the length of a 70 micron crack by about 15%, the crack size roughly doubles over the next 40,000 cycles. After 80,000 cycles the original flaws are on the verge of becoming visible and, more importantly, the residual fatigue lifetime is now very small. The small increment in flaw size that may subsequently be effected by ozone cracking during annealing consequently has a negligible effect on the ultimate properties (Figure 7).

Fatigue Life Improvement

The loss of failure properties at low annealing strains is seen to result from ozone induced growth of inherent flaws. At higher strains (>20%) the high concentration of microcracks that develops causes relaxation of stress at the surface of the material whereby there is less effective elevation of the stress at the flaw tips. However, after annealing at very high strains (> 100%), the fatigue life and tensile strength of the NR and IR stocks attain a level exceeding that of the initial, unfatigued, samples (see, for example, Table III and Figures 1 and 2). Since the bulk properties are not affected by the annealing (Table V), the changes in failure properties can be attributed to either a change in the stress concentration about an existing flaw or to a change in the material in proximity to the flaw. The surface effects induced by low strain annealing can not be expected to provide failure properties better than those of an unannealed sample. The improvements at the higher annealing strain are therefore of different origin than the low strain phenomena occasioned by ozone stress cracking.

When a non-crystallizing rubber is subjected to the higher annealing strains, no increase in strength over the unannealed rubber is realized (Figure 5 for SBR-1). This suggests that strain induced crystallization at the crack tip is responsible for the superior performance of the NR and IR compounds after annealing at high strains. When either of the unfilled polyisoprene based rubbers was stretched, up through about 500%

elongation the resulting elastic stress was found to be in accord with the Mooney-Rivlin description of the strain dependence of this stress [10]. Beyond this extension, the equilibrium stresses were significantly less than the values extrapolated from the lower strain results. A tensile elongation of 500% was also found to be the minimum necessary for observation of the x-ray reflection pattern associated with oriented crystallinity. This apparent absence of bulk crystallinity at an annealing strain of circa 100%, however, does not preclude local crystallization at the tip of a crack. Amplification of the strain in the vicinity of the tip of a 70 micron crack would be sufficient to effect localized strains in excess of 500% for a bulk strain of 100% [17].

Such crystallization is not completed during the brief residence at the peak strains during fatigue cycling. This fact can be gleaned from Figure 9, in which the relaxation time measured for the NR-2 is displayed versus strain. At strains for which orientational crystallization takes place, there is a large increase in the apparent relaxation time. This reflects the time scale of the crystallization process, which can be seen to continue well beyond the time scale of a dynamic fatigue cycle. As a result annealing at high strain allows extensive crystallization in the crack tip region with consequent improvement in failure properties.

More persuasive evidence that strain crystallization is the relevant mechanism is obtained if after the annealing the sample

is heated for a few minutes to at least 100°C. If the heating is done in the unstrained state, the fatigue life (Table III) or tensile strength (Table VI) is observed to return to the level measured for unannealed specimens. This temperature is sufficient to melt the crystallites at the crack tip, at least when the sample is unstrained. If the strain is maintained during the heating, the reference state with regard to the thermodynamic stability of the crystallites is a highly oriented amorphous state. Under these conditions it is expected that the crystal phase will exhibit greater stability; that is, it possesses a melting point higher than 100°C.

It is conceivable that during annealing at high strain there might be sufficient additional relaxation of stress, such that the crack growth during subsequent fatigue cycling would be slower due to a reduced strain energy density. In fact the heating experiments described above are not inconsistent with such an interpretation. The non-crystallizing SBR, however, would also benefit from such a mechanism, since its relaxation times were measured to be of the same order of magnitude as that of the polyisoprene stocks. It was also determined, moreover, that if the measurements were made not immediately after annealing, but rather 24 hours later (with the specimens in an unstrained in the interim), the fatigue life or tensile strength exhibited the same increase over unannealed samples. Finally, it is noted that at room temperature tensile retraction prior to straining to failure does not increase the breaking stress of

polyisoprene rubbers, notwithstanding the relaxation transpiring therein [20]. These results indicate that the increase in properties at the higher annealing strains is a consequence of strain induced crystallization.

SUMMARY

Annealing of polyisoprene based elastomers can result in improvement or in deterioration of its failure properties, depending on the deformation of the rubber during the annealing. These alterations in performance, moreover, are readily induced at strains within the range of conventional fatigue and crack growth experimentation. Although the effects of annealing on the behavior of rubber described herein represent manifestations of well known phenomena, they demonstrate the difficulties in relating laboratory characterizations to the performance of materials in other environments. This difficulty is emphasized by our observation of ozone induced crack growth in test specimens exposed to ambient air.

ACKNOWLEDGEMENTS

The authors express their appreciation to Mr. J.P. Armistead, of NRL, for assistance with the microscopy work, and to Mr. E. Greenawald, of Geo-Centers Inc., who implemented the modification of the Fatigue Tester. This work was supported in part under Office of Naval Research Contract No. N0001488WX24207.

REFERENCES

1. R.S. Rivlin and A.G. Thomas, J. Polym. Sci. 10, 291 (1953).

2. G.J. Lake and A.G. Thomas, Proc. Roy. Soc. 300, 108 (1967).

3. A.N. Gent in "Science and Technology of Rubber", Chap. 10. (F.R. Eirich, ed.), Academic Press, New York, 1978.

4. G.J. Lake, Rub. Chem. Tech. 45, 309 (1972).

5. C.M. Roland and C.R. Smith, Rub. Chem. Tech. 58, 806 (1985).

6. V.S. Kuksenko and V.P. Tamuzs, "Fracture Micromechanics of Polymer Materials", Martinus Nijhoff, The Hague, 1981.

7. A. Chudnovsky, I. Palley, and E. Baer, J. Matl. Sci. 16, 35 (1981).

8. A. Chudnovsky, and A. Moet, Polym. Eng. Sci. 22, 922 (1982).

9. G.J. Lake and P.B. Lindley, J. Appl. Polym. Sci.

10. C.M. Roland, J. Rheology, submitted.

11. J.I. Cunneen, Rub. Chem. Tech. 41, 182 (1968).

12. A.A. Popov and G.E. Zaikov, J. Macro. Sci. - Rev. Macro. Chem. Phys. C23, 1 (1983).

13. J.R. Beatty, Rub.Chem. Tech. 37, 1341 (1964).

14. M. Braden and A.N. Gent, J. Appl. Polym. Sci. 3, 90 (1960).

15. M. Braden and A.N. Gent, J. Appl. Polym. Sci. 3, 100 (1960).

16. G.J. Lake and P.B. Lindley, J. Appl. Polym. Sci. 9, 2031 (1965).

17. K. Hellan, "Introduction to Fracture Mechanics", McGraw Hill, New York, 1984.

18. A.G. Thomas and J.M. Whittle, Rub. Chem. Tech. 43, 222 (1970).

19. C.L.M. Bell, D. Stinson, and A.G. Thomas, Rub. Chem. Tech. 55, 66 (1982).

20. J.A.C. Harwood and A.R. Payne, J. Appl. Polym. Sci. 11, 1825 (1967).

TABLE I

Rubber Compositions

Designation	NR-1	NR-2	NR-3	IR-1	SBR-1
NR	100	100	100	--	--
IR	--	--	--	100	--
SBR	--	--	--	--	100
N-326	45	--	60	--	--
antioxidant	0.5	0.5	0.5	0.5	--
dicumyl peroxide	--	1.0	1.2	1.0	0.1
zinc oxide	3	--	--	--	--
stearic acid	2	--	--	--	--
sulfur	3	--	--	--	--
accelerator	1	--	--	--	--

TABLE II

Effect of Unstrained Annealing on Fatigue Behavior of NR-1

Precycles	Annealing Time (min)	Fatigue Lifetime (cycles)
----	0	101,000
22,000	2805	97,000
37,000	961	101,000

TABLE III

Effect of Annealing on Fatigue Behavior

of IR-1 (Dynamic Strain = 124%)

Precycles[a]	Annealing Strain	Annealing Time (min)	Fatigue Lifetime (cycles)
---	---	--	156,000
200	12	1440	90,000
"	124	"	206,000
"	12	2880	46,000
"	124	"	170,000
40,000	---	--	154,000
"	12	1440	142,000
"	124	"	170,000
"	12	4320	77,000
"	124	"	203,000
"	12	" [b]	82,000[b]
"	124	" [b]	267,000[b]
"	12	" [c]	64,000[c]
"	124	" [c]	147,000[c]
"	0	" [d]	189,000[d]
"	12	" [d]	184,000[d]

[a] Number of fatigue cycles prior to annealing.

[b] After annealing specimens heated to 110°C in strained state immediately prior to resumption of fatigue cycling.

[c] After annealing specimens heated to 110°C in unstrained state immediately prior to resumption of fatigue cycling.

[d] Annealing executed in vacuum at room temperature.

TABLE IV

Effect of Annealing on Fatigue Behavior of Natural Rubber Based Stocks

(Precycles = 200, Dynamic Strain = 124%)

Stock	Annealing Strain	Annealing Time (min)	Fatigue Lifetime (cycles)
NR-2	12	4320	56,000
NR-2	124	"	179,000
NR-3	---	0	54,000
NR-3	12	4320	45,000
NR-3	124	"	55,000

TABLE V

Effect of Annealing on Equilibrium Swelling (in Cyclohexane) and Optical Density

Sample	Swelling Ratio	Transmission (at 500 nm)
NR-2 unannealed	0.16	12%
NR-2 annealed 72 hrs at 124% strain	0.16	1%
SBR-1 unannealed	0.17	15%
SBR-1 annealed 72 hrs at 124% strain	0.16	3%

TABLE VI

Effect of Annealing on Tensile Strength

for Natural Rubber Based Stocks

(72 Hours at 124% Elongation)

Annealed	Heated	Tensile Strength (MPa)
No	----	15.9
Yes	----	17.3
Yes	Strained	18.0
Yes	Unstrained	16.0

FIGURE CAPTIONS

Figure 1: The influence of annealing for 24 hours at various strains on the fatigue lifetime of IR-1. The results for each individual test specimen are shown in order to demonstrate that the decrease at low annealing strain, as well as the improvement at higher annealing strain, exceed the experimental scatter in the measurements.

Figure 2: The tensile strength of NR-2 after annealing for 72 hours at the indicated elongation. The results, each representing the average of eight measurements, had an average deviation of about one megapascal.

Figure 3: Stress relaxation in NR-2 during a reversing double step strain. The initial extension was 135% (+++) for 2 min followed by a 10% strain and (***) for 120 min followed by a 5% strain. Zero on the abscissa corresponds to the time at which the second step was imposed.

Figure 4: The tensile strength of IR-1 after annealing for 72 hours at the indicated strain.

Figure 5: The effect of annealing (for 72 hours) of SBR-1 at the indicated tensile strains on the subsequently measured stress at break. Although the data for duplicate testing were not normally distributed, a standard deviation of 0.05 MPa was calculated.

Figure 6: Scanning electron micrographs of the surface damage accumulating in NR-2 after (a) 72 and (b) 288 hours of annealing in air at 124% elongation (the scale mark indicates 20 microns). As can be seen in these edge views, the region of pervasive microcracking extends about 30 microns into the bulk of the material.

Figure 7: The effect on the tensile strength of annealing NR-2 at various strains. The 72 hour annealing period commenced after (*) 200, (o) 40,000, and (●) 80,000 fatigue cycles at 124% elongation.

Figure 8: The relationship between the tensile strength of NR-2 and the length of an edge precrack. From the tensile strength measured for samples without intentionally introduced cuts (designated by the horizontal dotted line), the inherent flaw size is estimated to be about 70 microns.

Figure 9: The time period required for cessation of stress relaxation in NR-2 as a function of the uniaxial extension ratio. The increases at the higher strains, which coincide with deviations in the strain dependence of the elastic modulus from the Mooney-Rivlin theory, are associated with the onset of orientational crystallization.

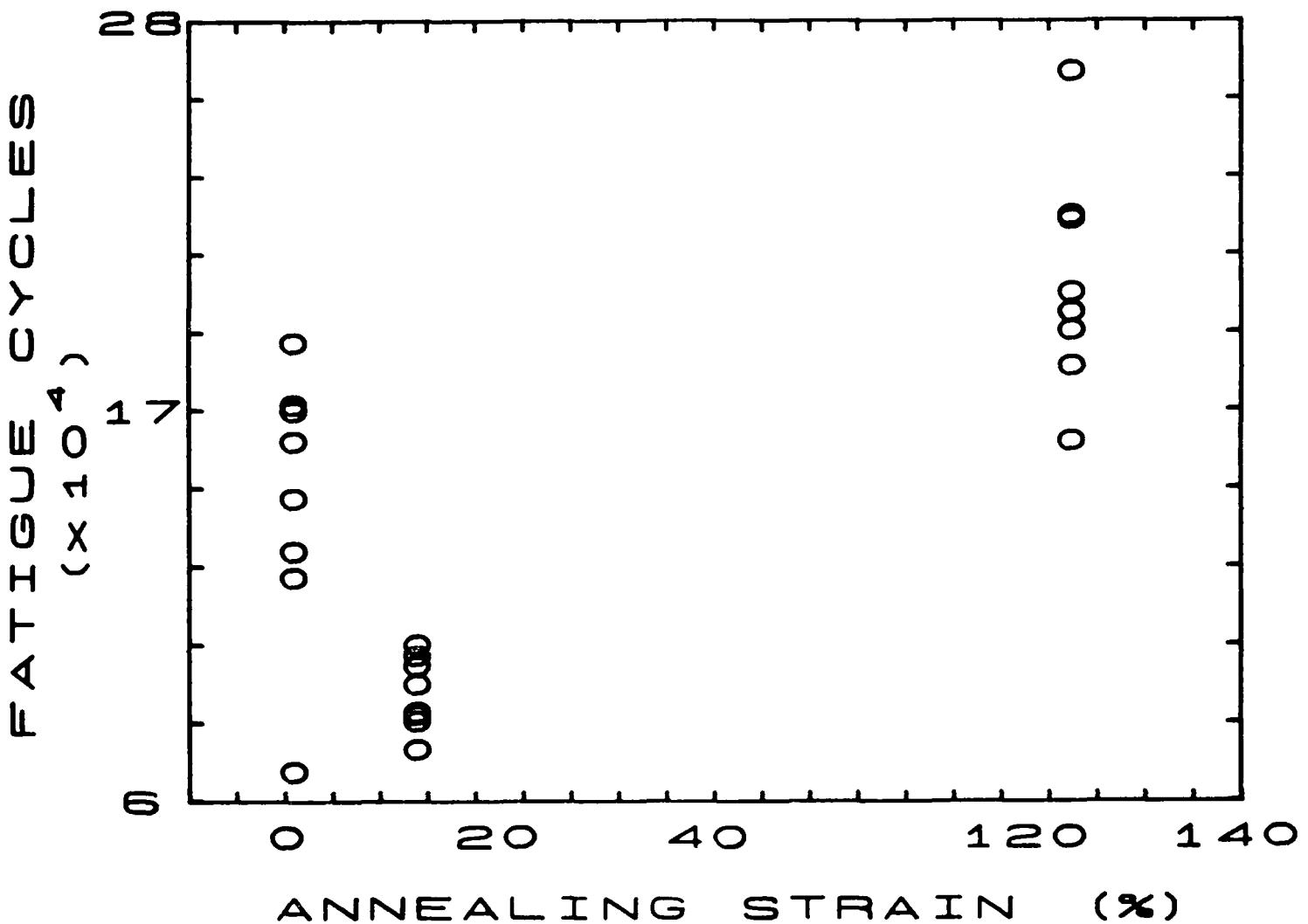
28
17
6
FATIGUE CYCLES
(X10^4)
0
20
40
120
140
ANNEALING STRAIN (%)

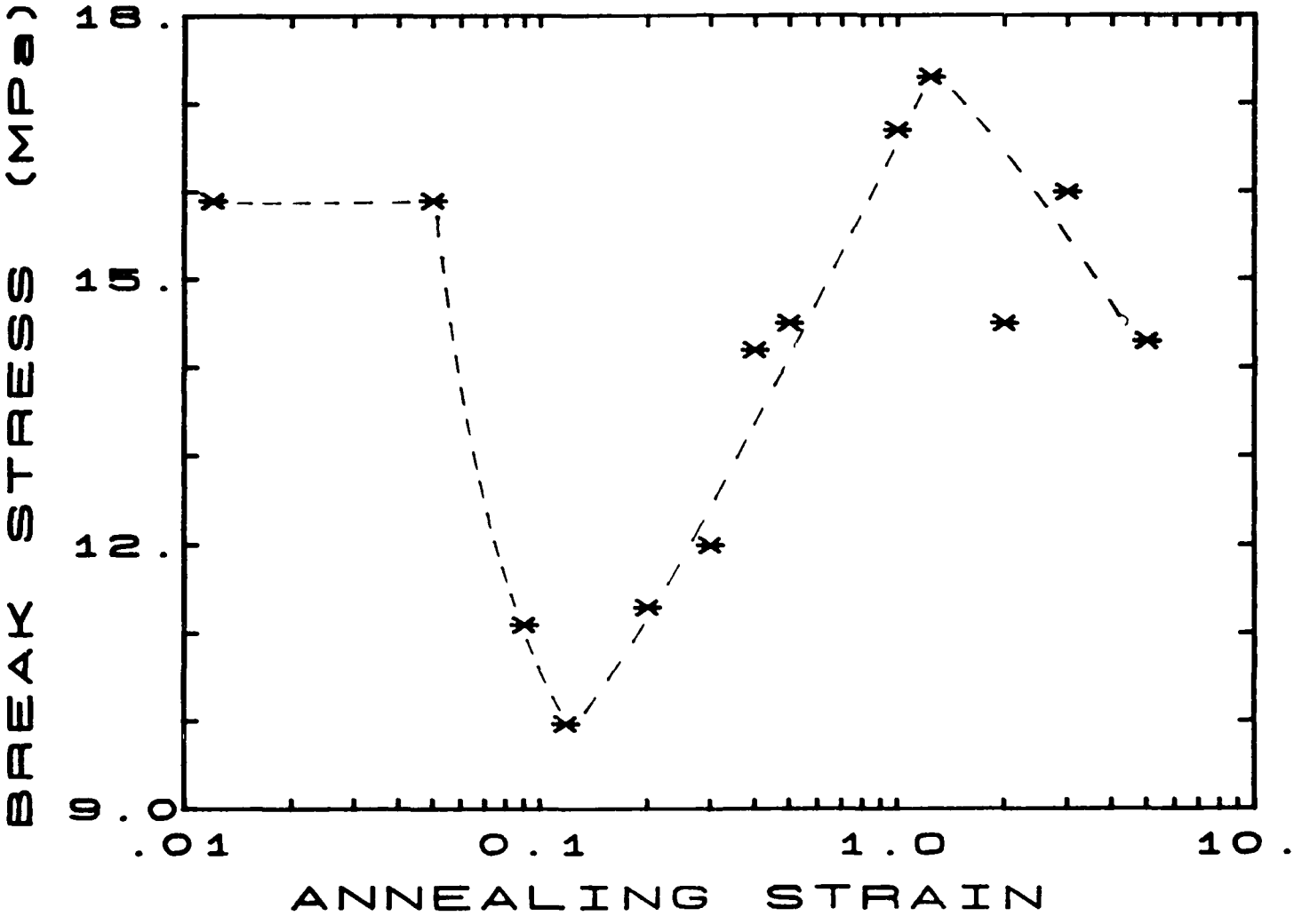
BREAK STRESS (MPa)
18.
15.
12.
9.0
.01
0.1
1.0
10.
ANNEALING STRAIN

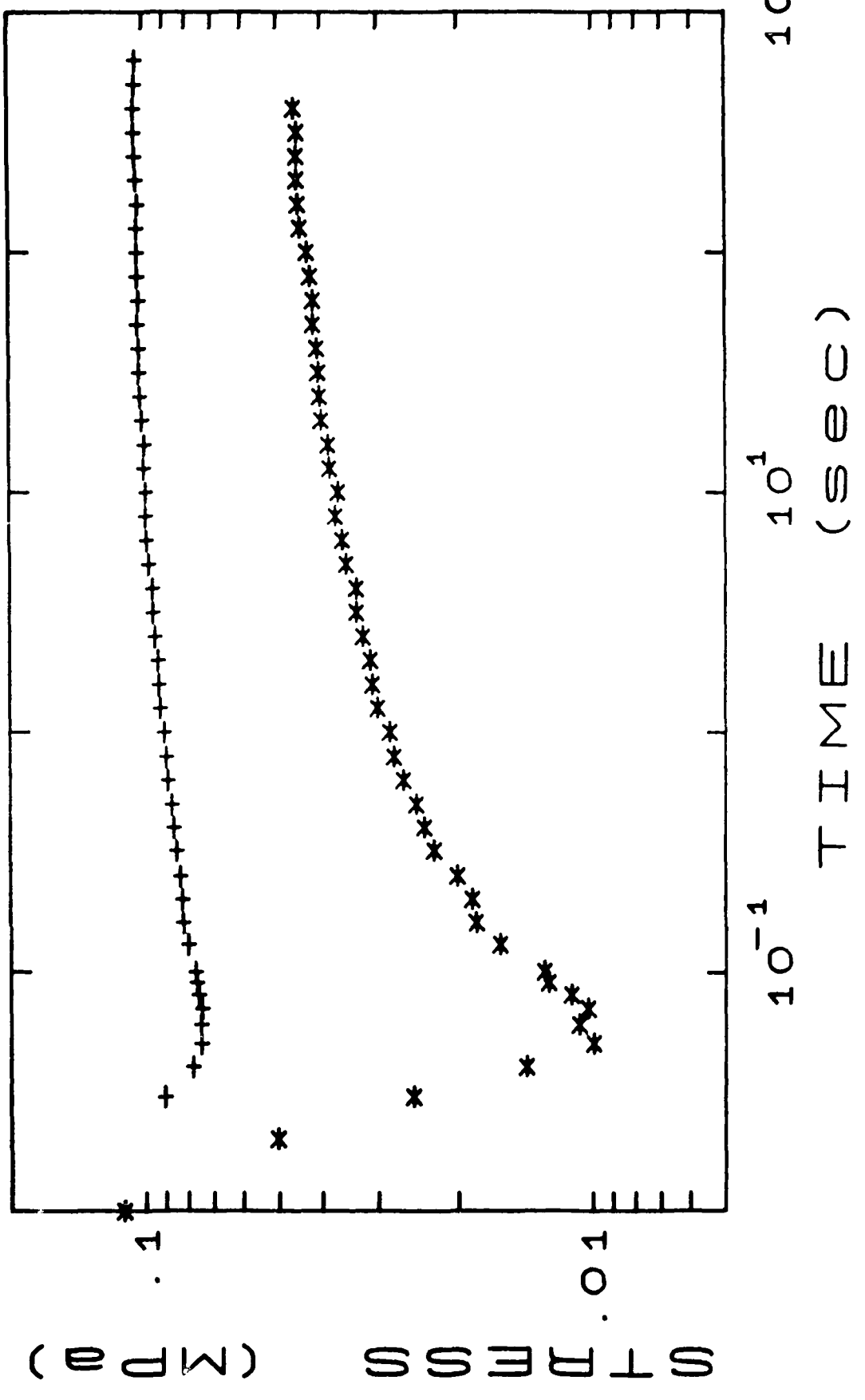
STRESS (MPa)
1.
0.1
TIME (sec)
10^{-1}
10^{1}
10^{3}

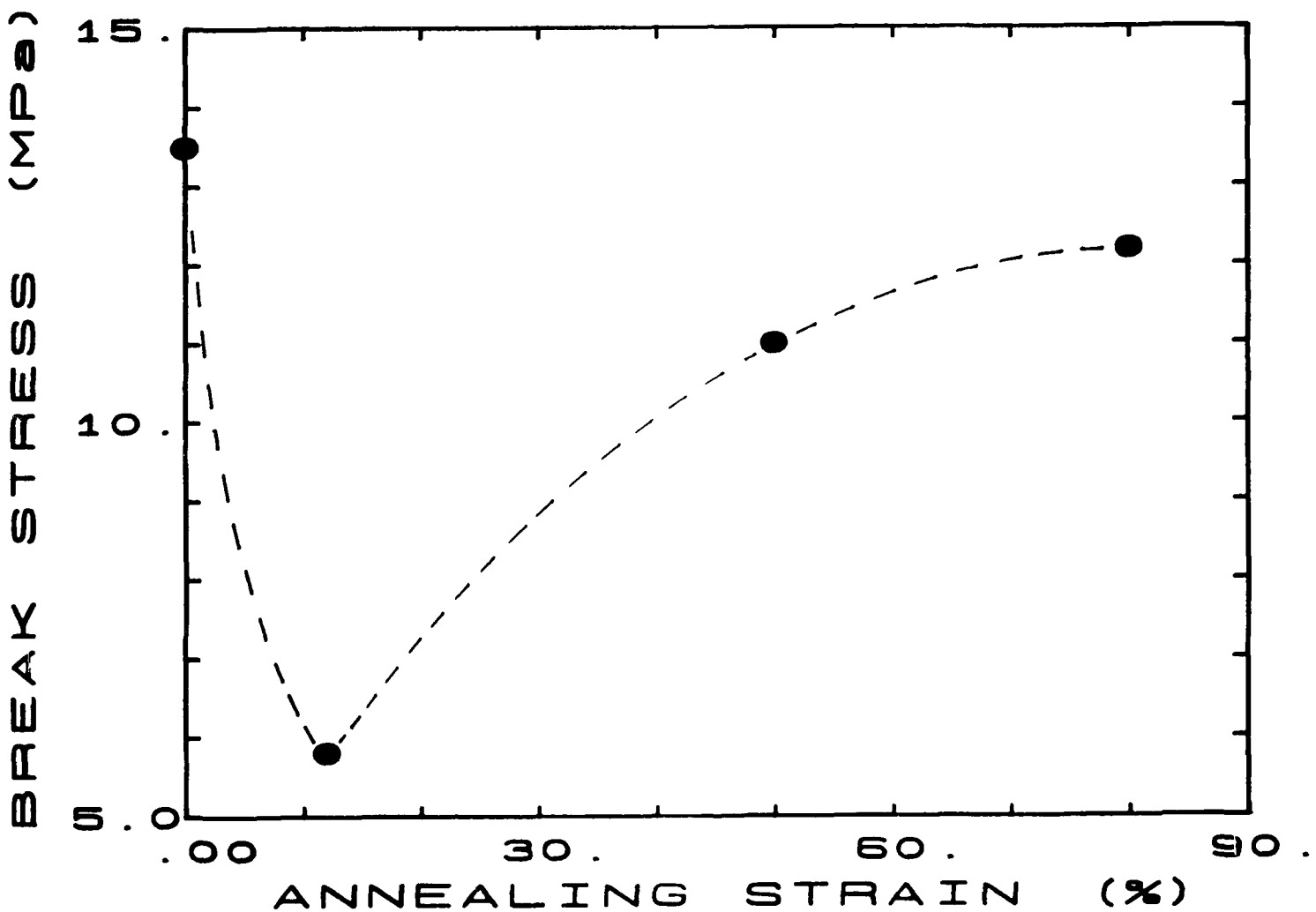
BREAK STRESS (MPa)
15.
10.
5.0
.00
30.
60.
90.
ANNEALING STRAIN (%)

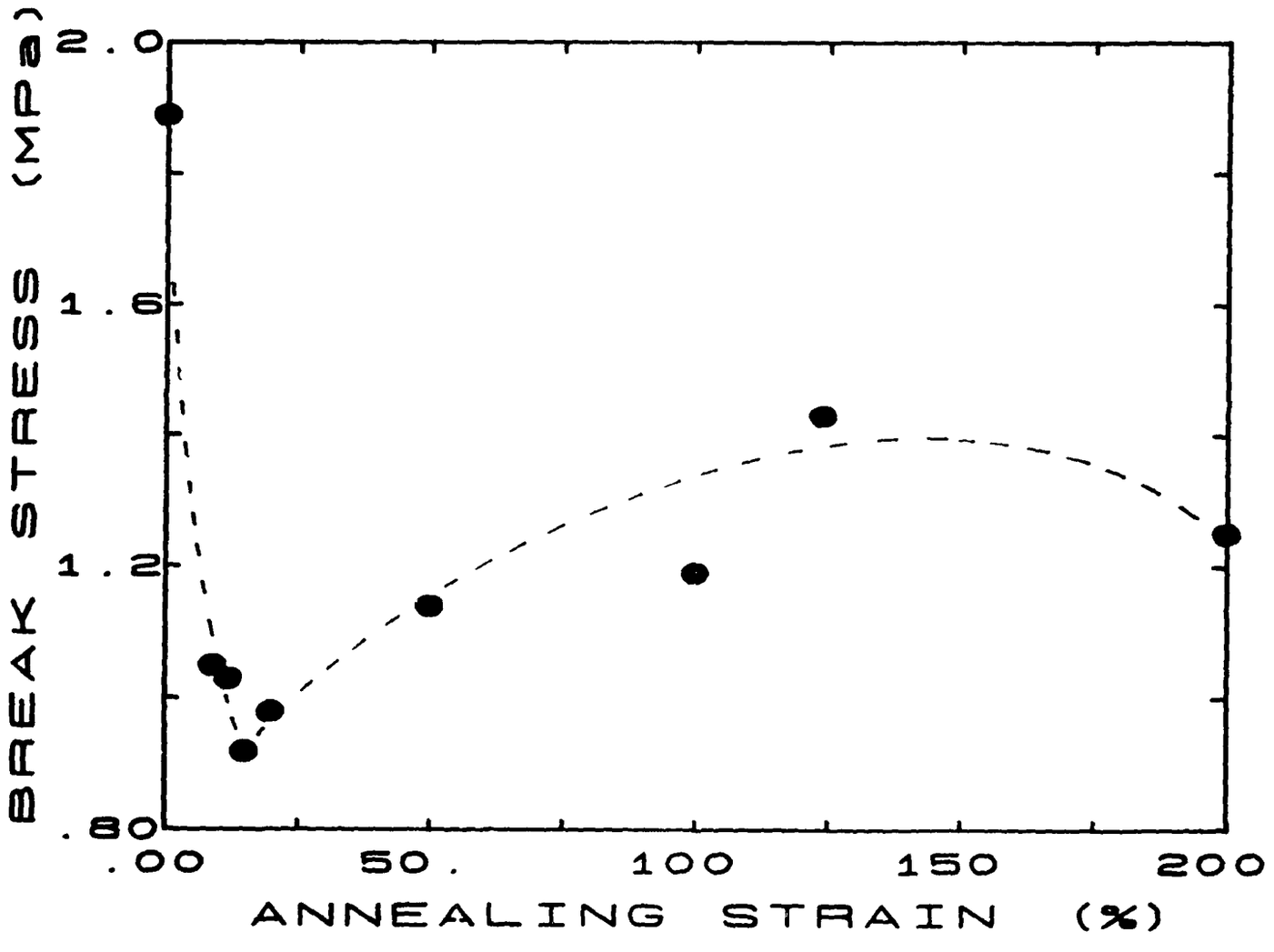
BREAK STRESS (MPa)
2.0
1.6
1.2
.80
.00
50.
100
150
200
ANNEALING STRAIN (%)

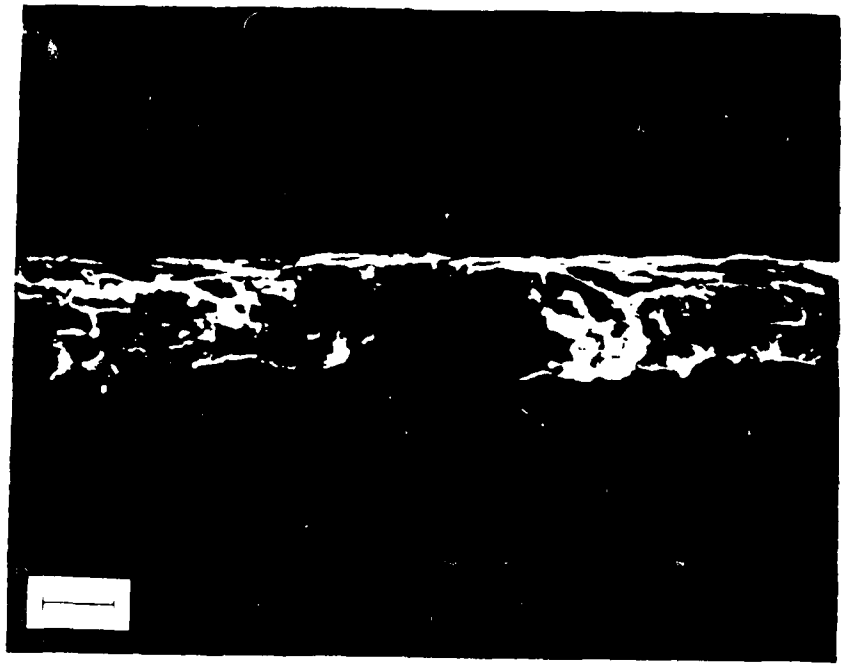

A

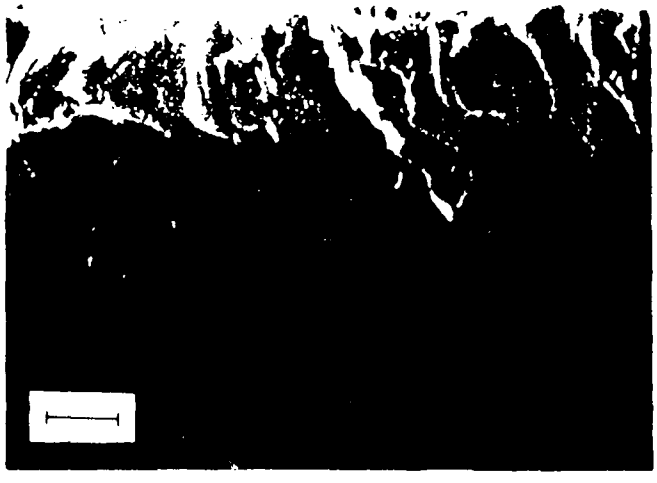

B

FIG 6

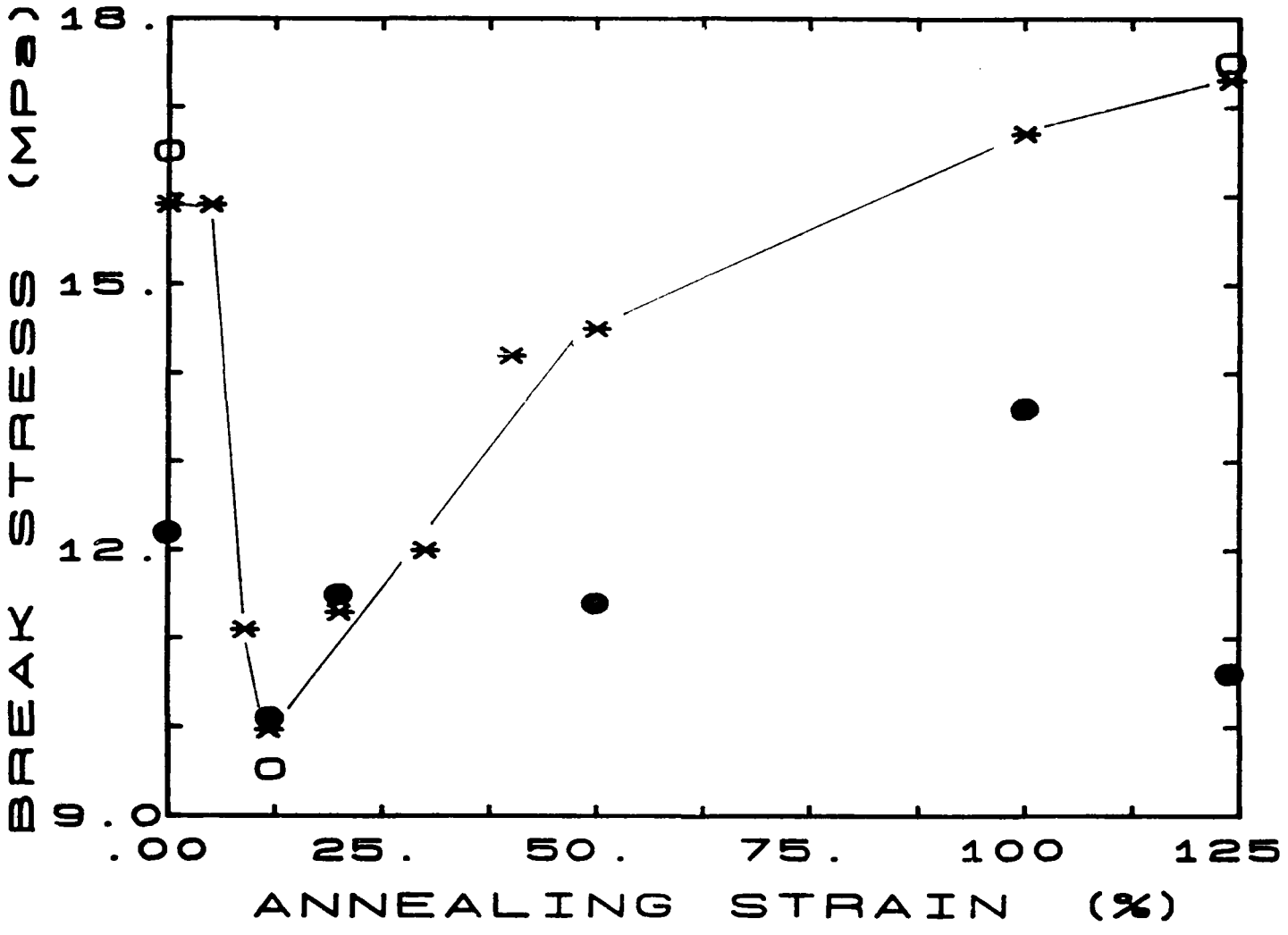
BREAK STRESS (MPa)
18.
15.
12.
9.0
.00
25.
50.
75.
100
125
ANNEALING STRAIN (%)

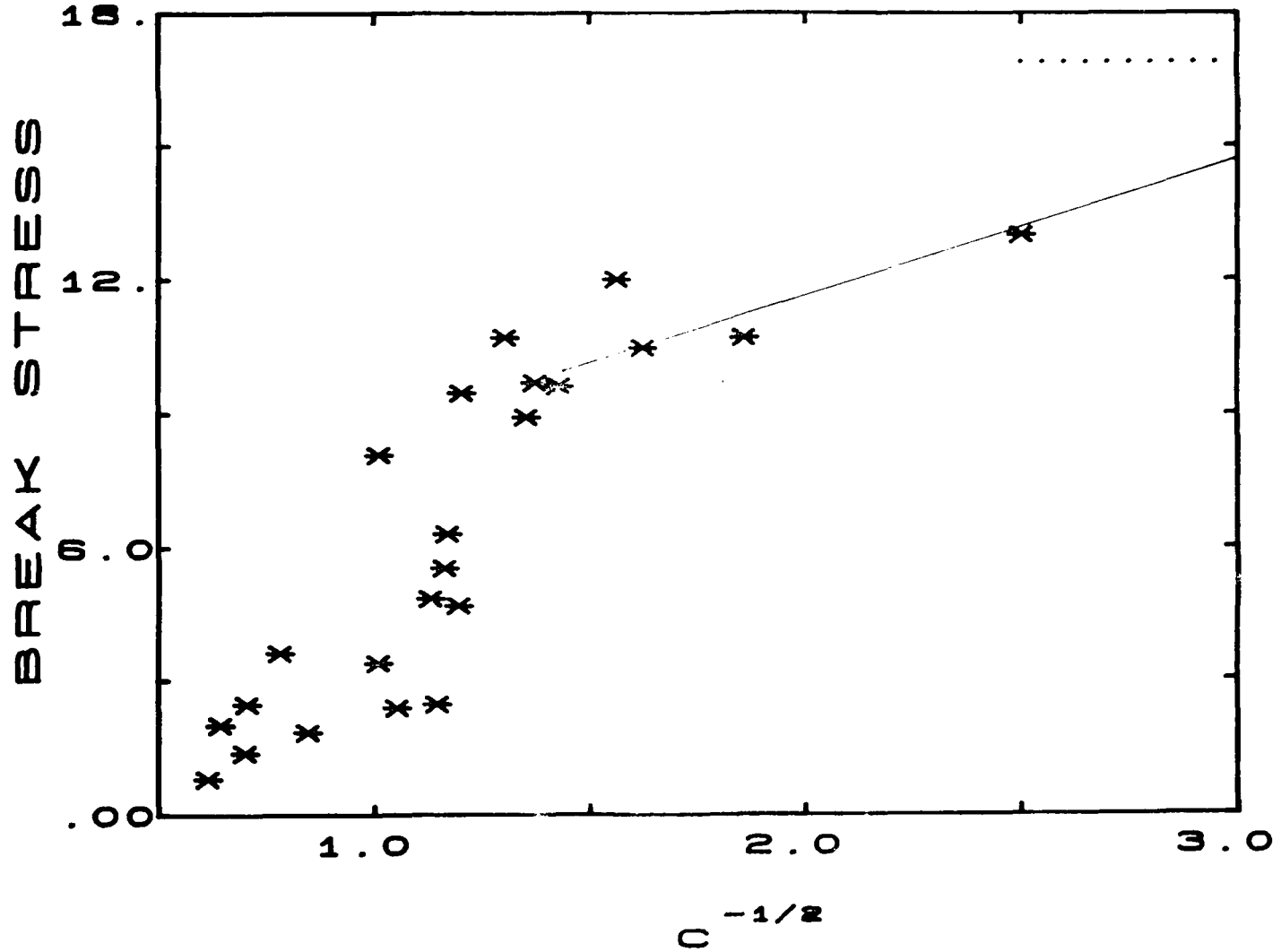
18.
12.
6.0
.00
BREAK STRESS
1.0
2.0
3.0
C -1/2

TECHNICAL REPORT DISTRIBUTION LIST, GEN

	No. Copies
Office of Naval Research Attn: Code 1113 800 N. Quincy Street Arlington, VA 22217-5000	2
Dr. Bernard Douda Naval Weapons Support Center Code 50C Crane, IN 47522-5050	1
Naval Civil Engineering Laboratory Attn: Dr. R. W. Drisko, Code L52 Port Hueneme, CA 93401	1
Defense Technical Information Center Building 5, Cameron Station Alexandria, VA 22314	12 (high quality)
DTNSRDC Attn: Dr. H. Singerman Applied Chemistry Division Annapolis, MD 21401	1
Dr. James S. Murday Superintendent Chemistry Division, Code 6100 Naval Research Laboratory Washington, DC 20375-5000	1
Dr. David Young Code 334 NORDA NSTL, Mississippi 39529	1
Naval Weapons Center Attn: Dr. Ron Atkins Chemistry Division China Lake, CA 93555	1
Scientific Advisor Commandant of the Marine Corps Code RD-1 Washington, DC 20380	1
U.S. Army Research Office Attn: CRD-AA-IP P.O. Box 12211 Research Triangle Park, NC 27709	1
Mr. John Boyle Materials Branch Naval Ship Engineering Center Philadelphia, PA 19112	1
Naval Ocean Systems Center Attn: Dr. S. Yamamoto Marine Sciences Division San Diego, CA 91232	1